Citation (APA)
Liu, J., Yang, Q., Zhang, Y., Wang, S., Wei, W., Su, W., & Wu, R. (2025). Physicochemical characterisation of severely aged crumb rubber modified bitumen. *Frontiers in Materials*, *12*, Article 1741288.
https://doi.org/10.3389/fmats.2025.1741288

frontiers | Frontiers in Materials

TYPE Original Research
PUBLISHED 12 December 2025
DOI 10.3389/fmats.2025.1741288

Check for updates

OPEN ACCESS

EDITED BY
Augusto Cannone Falchetto,
University of Padua, Italy

REVIEWED BY
Fan Zhang,
Aalto University, Finland
Bhaswati Bora,
University of Padua, Italy

*CORRESPONDENCE
Rui Wu,
r.wu-2@tudelft.nl

RECEIVED 07 November 2025
REVISED 26 November 2025
ACCEPTED 29 November 2025
PUBLISHED 12 December 2025

CITATION
Liu J, Yang Q, Zhang Y, Wang S, Wei W, Su W and Wu R (2025) Physicochemical characterisation of severely aged crumb rubber modified bitumen.
Front. Mater. 12:1741288.
doi: 10.3389/fmats.2025.1741288

Physicochemical characterisation of severely aged crumb rubber modified bitumen

Jiayao Liu[1], Qian Yang[1], Yan Zhang[1], Shaokun Wang[1], Wei Wei[1], Wenbin Su[2] and Rui Wu[3]*

[1]College of Civil Engineering, Shaanxi Polytechnic University, Xianyang, China, [2]School of Highway, Chang'an University, Xi'an, China, [3]Faculty of Civil Engineering and Geosciences, Delft University of Technology, Delft, Netherlands

Crumb rubber was incorporated into neat bitumen at a dosage of 15 wt% to mitigate the challenges of rising crude oil prices, high dependence on fossil fuels, and energy shortages. Both the unmodified bitumen and crumb rubber modified bitumen (CRMB) were subjected to short- and severe long-term ageing. The rheological properties were evaluated using a dynamic shear rheometer (DSR) and a bending beam rheometer (BBR) to investigate the high-, intermediate-, and low-temperature performance of the binders under different ageing conditions. Fourier-transform infrared spectroscopy (FTIR) was employed to characterise the chemical changes with modification and ageing. The results indicate that the incorporation of crumb rubber significantly enhances the high- and low-temperature performance of bitumen but slightly reduces its fatigue resistance and durability. Crumb rubber does not alter the oxidation pathway of bitumen. After severe long-term ageing, the chemical characteristics of CRMB remain comparable to those of neat bitumen.

KEYWORDS

ageing, crumb rubber modified bitumen, durability, fatigue, rheology

1 Introduction

Asphalt pavements account for over 90% of road surfaces worldwide (EAPA, 2025). In some countries, such as the United States, this proportion reaches approximately 94% (NAPA, 2020), underscoring their vital role in societal and economic development. Bitumen serves as the binding material in asphalt pavements, providing cohesion among aggregates and contributing to the overall strength of asphalt mixtures. Over the past two centuries, bitumen has been extensively used as the primary pavement binder (Li et al., 2024). Although recent research has explored bio-based alternatives from a sustainability perspective (Espinosa et al., 2024; Hu et al., 2025c; Cannone Falchetto et al., 2025), bitumen remains the dominant construction binder (Zhang et al., 2025b). Global demand for bitumen continues to grow due to the expansion of road networks, increasing needs for infrastructure maintenance and renewal, and the pursuit of longer-lasting pavements (Sun et al., 2026; Zhang et al., 2025a). However, bitumen is a petroleum-derived, non-renewable material, making its long-term availability a pressing concern (Shi et al., 2024; Wang et al., 2025). The depletion of crude oil reserves, coupled with competition from other petroleum-based industries, has led to price volatility and a sustained increase in bitumen costs. Compared with 2010, current prices have nearly tripled (GDoT, 2025; MAA, 2024). This escalation not only raises construction and maintenance costs but also underscores the urgency of developing sustainable alternatives or partial replacements (Hu et al., 2025b; Patel et al., 2025).

Meanwhile, rapid urbanisation and the rising demand for logistics have dramatically increased the number of vehicles, including cars and heavy lorries. Consequently, over one billion tonnes of waste tyres are generated annually (WBCSD, 2010). Improper disposal methods, such as open burning or landfilling, pose serious environmental risks. To mitigate these issues, the recycling and reuse of waste tyres have attracted growing attention from both academia and industry. One of the most promising and practical recycling approaches is using waste tyres to modify bitumen, thereby enhancing the sustainability and resilience of road infrastructure.

Typically, waste tyres are pretreated to remove steel and textile cords, then mechanically ground into powder or small particles before being incorporated into bitumen as a modifier. These rubber particles, termed crumb rubber, are blended with bitumen to produce crumb rubber modified bitumen (CRMB). Tyre-derived crumb rubber mainly consists of natural rubber (about 45%–50% by weight) and approximately 20% carbon black, along with small amounts of metal oxides, sulphur, textiles, and other additives (Wang, 2021). The natural rubber contributes elasticity, improving resistance to permanent deformation, while the carbon black enhances ageing resistance (Wang et al., 2020b).

During the blending process, interactions between crumb rubber and bitumen primarily involve swelling and degradation. In the swelling phase, light components of bitumen, such as saturates and aromatics, diffuse into the rubber matrix at high temperatures, causing volume expansion and the formation of a gel layer at the rubber–bitumen interface (Wang, 2021). This diffusion absorbs the bitumen of light, flexible fractions, leading to stiffening. In general, rubber swelling has three effects on the properties of bitumen: (a) changing the component proportions due to absorption of maltenes, (b) changing the microstructure of bitumen, and (c) stiffening bitumen due to the inclusions of crumb rubber particles with increased volume (Wang, 2021).

Additionally, at high temperatures and shear rates, the crosslinked rubber structure partially breaks down, releasing polymer chains into the bitumen and improving CRMB's storage stability (Lo Presti et al., 2018; Shi et al., 2025). Previous studies have demonstrated that incorporating crumb rubber can significantly enhance rutting resistance, fatigue life, and thermal cracking resistance (Kumar et al., 2020), highlighting its potential in sustainable pavement engineering.

However, like all organic materials, bituminous binders, including CRMB, are susceptible to ageing. Numerous studies have investigated the ageing mechanisms of unmodified bitumen. During ageing, the relative proportions of the four main bitumen fractions, namely saturates, aromatics, resins, and asphaltenes (SARA) change substantially. Aromatics typically decrease, resins increase markedly, and asphaltenes in-crease slightly but critically, while saturates remain nearly constant (Hu et al., 2025e). These compositional shifts disturb the colloidal stability of bitumen, enhancing polarity, promoting asphaltene agglomeration, and forming oxygen-containing functional groups such as carbonyls and sulfoxides (Hu et al., 2025d; Hu et al., 2024d). Consequently, bitumen becomes stiffer and more brittle, with higher viscosity, complex modulus, and softening point but lower ductility, phase angle, and penetration (Gao et al., 2021). Such changes in physicochemical properties deteriorate pavement performance, leading to distresses such as cracking and pothole formation.

Despite extensive research on the ageing of neat bitumen, studies on the ageing behaviour of CRMB remain limited. Due to the swelling and degradation of rubber, CRMB exhibits distinct ageing characteristics and mechanisms. Understanding these mechanisms is essential to promote the broader and more effective application of CRMB, thereby advancing the sustainability and durability of road infrastructure. In this context, the present study systematically investigates the ageing behaviour of CRMB and provides insights that support its wider adoption in the pavement sector.

2 Objective and approaches

This study aims to investigate the effects of ageing on the physicochemical properties of crumb rubber modified bitumen (CRMB). Both the reference bitumen and CRMB were subjected to short-term, and long-term ageing under different durations. Fourier-transform infrared (FTIR) spectroscopy was employed to identify changes in functional groups during the ageing process. The dynamic shear rheometer (DSR) was used to evaluate the rheological behaviour of bitumen. Frequency sweep (FS), linear amplitude sweep (LAS), and multiple stress creep and recovery (MSCR) tests were conducted to characterise the overall rheological response, fatigue performance, and high-temperature properties of the binders. In addition, the bending beam rheometer (BBR) test was performed to assess the low-temperature performance of bitumen.

3 Materials and methods

3.1 Materials

The reference binder used in this study was a 70/100 penetration grade unmodified bitumen, with a penetration of 83 dmm and a softening point of 46.0 °C. The crumb rubber was obtained from scrapped lorry tyres and had a nominal particle size of 0.2–0.8 mm. The crumb rubber modified bitumen (CRMB) was prepared in the laboratory using the reference bitumen, with a crumb rubber dosage of 15 wt%. The penetration and softening point of CRMB were 53 dmm and 50.5 °C, respectively.

3.2 Sample preparation and conditioning

Neat bitumen was preheated to 180 °C, subsequently the crumb rubber was added to the bitumen at the dosage of 15 wt%. The mix was blended on a laboratory hotplate at 180 °C for 45 min at 5,000

Abbreviations: CRMB, Crumb rubber modified bitumen; MSCR, Multiple stress creep and recovery; LAS, Linear amplitude sweep; J_{nr}, Nonrecoverable compliance; %R, Recovery percentage; $T_{C,S}$, Critical temperature controlled by stiffness; $T_{C,m}$, Critical temperature controlled by m-value; ΔT_C, Difference between $T_{C,S}$ and $T_{C,m}$; G-R parameter, Glover-Rowe parameter; N_f, Fatigue life; 2S2P1D, Two springs, two parabolic creep elements and one dashpot; AVOVA, Analysis of variance.

r/min using a high-speed shear mixer. Afterwards, the CRMB was subjected to ageing conditioning.

The short-term ageing of neat bitumen followed the standard rolling thin film oven (RTFO) ageing procedure as per ASTM D2872-22, consisting of 85 min of conditioning at 163 °C with air flow of 4 L/min (ASTM, 2022). However, the viscosity of CRMB was too high, making it difficult to properly cover the surface of jars for RTFO. Previous studies have reported that using the 140 mm diameter pan with 20 g of bitumen (1.25 mm thickness of the bitumen film) at 163 °C can reach a comparable short-term ageing effect of RTFO based on comparisons of carbonyl index, viscosity growth, mass loss, and complex modulus between binders aged using RTFO and those aged using the pan approach (Wang et al., 2020a). Therefore, this alternative short-term ageing protocol was adopted in this study. For the long-term ageing, both short-term aged bitumen residue was subjected to pressure ageing vessel (PAV) at 100 °C for 20 h, 30 h and 40 h.

3.3 Testing programme

Frequency sweep (FS) tests were conducted to evaluate their overall rheological properties. The testing temperatures ranged from 70 °C to 10 °C in 10 °C increments, and the frequency range was 0.1–100 rad/s, with 31 data points per temperature. For tests conducted between 70 °C and 40 °C, 25 mm parallel plates with a 1 mm gap were used, whereas for tests between 40 °C and 10 °C, 8 mm plates with a 2 mm gap were employed. The strain levels were set at 0.8% for unaged samples, 0.5% for short-term aged samples, and 0.2% for long-term aged samples, as determined from a preliminary amplitude sweep test. For each sample, two replicates were tested.

Multiple stress creep and recovery (MSCR) tests were performed at 70 °C to assess the high-temperature performance of both CRMB and the reference binder, following ASTM D7405-24 (ASTM, 2024). In accordance with the ASTM D7405 standard, the testing temperature should be the same as the higher PG of the binders. Based on preliminary tests, the higher PG for both neat bitumen and CRMB was 70 °C, therefore 70 °C was selected as the testing temperature. The repeatability for MSCR test is fairly high, therefore, only one replicate was tested. The first 100 cycles at 0.1 kPa are for conditioning while the second 100 cycles are for data analysis. Bending beam rheometer (BBR) tests were carried out at −6, −12, −18, and −24 °C to evaluate low-temperature performance, in accordance with ASTM D6648-25 (ASTM, 2025), with two replicates per sample. Linear amplitude sweep (LAS) tests were conducted at 25 °C to evaluate binder fatigue performance, following AASHTO T391-20 standard (AASHTO, 2020), with three replicates per sample.

Fourier-transform infrared (FTIR) spectroscopy was used to evaluate the chemical evolution of bitumen during the ageing process. The tests were performed in attenuated total reflectance (ATR) mode using 24 scans, with a scanning resolution of 4 cm^{-1} over the wavenumber range of 4,000–400 cm^{-1} (Mirwald et al., 2025), with four replicates per sample as recommended by literature.

3.4 Data processing

3.4.1 Frequency sweep

Based on the results of frequency sweep tests, the limited measured data were extrapolated to generate extended results of interest. The frequency sweep data at all temperatures were shifted horizontally using the Williams–Landel–Ferry (WLF) equation to construct the master curve at the selected reference temperature. The 2S2P1D model was then fitted to the complex modulus master curve using a nonlinear least-squares optimisation procedure. Both the storage and loss components were fitted simultaneously to ensure consistency between the real and imaginary parts of the complex modulus. The optimisation was performed with physically reasonable bounds on all parameters ($0 < k < h < 1$, $\delta > 0$), and convergence was achieved for every binder and ageing condition with excellent agreement between measured and modelled values ($R^2 > 0.99$). The fitted master curves were subsequently used to obtain $|G^*|$ and δ at 15 °C and 0.005 rad/s for calculating the Glover–Rowe parameter. The master curve of the complex modulus was constructed using the 2S2P1D model, as expressed in Equation 1. The reference temperature for general analysis in this study was set at 25 °C, while 15 °C was used as the reference temperature for calculating the Glover–Rowe (G–R) parameter.

$$G^*(\omega) = G_0 + \frac{G_g - G_0}{1 + \delta(i\omega\tau)^{-k} + (i\omega\tau)^{-h} + (i\omega\beta\tau)^{-1}} \tag{1}$$

where G_0 is the static modulus, which equals zero for bituminous binders, and G_0 is the glassy modulus as $\omega \to \infty$. h and k are exponents within the range $0 < k < h < 1$, δ is a dimensionless constant, i is the complex number ($i^2 = -1$), and τ is the characteristic time, which varies with temperature.

The complex modulus (G^*) consists of two components: the real (storage) modulus (G') and the imaginary (loss) modulus (G''), as described in Equation 2.

$$G^*(\omega) = G'(\omega) + iG''(\omega) \tag{2}$$

Equation 2 can be rewritten as Equation 3.

$$G^* = \left[G_0 + \frac{\left(G_g - G_0\right) \times (1 + A)}{(1 + A)^2 + B^2} \right] + i \left[\frac{\left(G_g - G_0\right) \times (-B)}{(1 + A)^2 + B^2} \right] \tag{3}$$

where A and B are defined by Equations 4, 5, respectively.

$$A(\omega) = \delta(\omega\tau)^{-k} \times \cos\left(\frac{k\pi}{2}\right) + (\omega\tau)^{-h} \times \cos\left(\frac{h\pi}{2}\right) \tag{4}$$

$$B(\omega) = -(\omega\beta\tau)^{-1} - \delta(\omega\tau)^{-k} \times \sin\left(\frac{k\pi}{2}\right) - (\omega\tau)^{-h} \times \sin\left(\frac{h\pi}{2}\right) \tag{5}$$

The master curve for the phase angle was calculated using Equation 6:

$$\delta = \tan^{-1}\left(\frac{G''}{G'}\right) \tag{6}$$

The G–R parameter was determined using Equation 7, where G^* and the phase angle (δ) were derived from the master curves. The calculations were performed at a temperature of 15 °C and a frequency of 0.005 rad/s.

$$G - R = \frac{G^*(\cos\delta)^2}{\sin\delta} \tag{7}$$

3.4.2 Multiple stress creep and recovery tests

The strain response was recorded during testing. Based on the strain data, the nonrecoverable compliance (J_{nr}) at both stress levels was calculated using Equations 8–10. Each stress level consisted of ten loading–recovery cycles, and the final J_{nr} was taken as the average from these ten cycles at both 0.1 kPa and 3.2 kPa.

$$\varepsilon_{10} = \varepsilon_r - \varepsilon_0 \tag{8}$$

$$J_{nr0.1} = \frac{\varepsilon_{10}}{0.1} \tag{9}$$

$$J_{nr3.2} = \frac{\varepsilon_{10}}{3.2} \tag{10}$$

where ε_r is the strain at the end of the recovery phase and ε_0 is the strain at the beginning of the creep phase for the corresponding stress level.

The difference in J_{nr} between the two stress levels ($J_{n_r\text{-}diff}$) was calculated using Equation 11.

$$J_{nr-diff} = \frac{J_{nr3.2} - J_{nr0.1}}{J_{nr0.1}} \times 100\% \tag{11}$$

The recovery percentage was computed using Equation 12, also averaged over ten cycles for both stress levels.

$$\%\mathrm{R} = \frac{\varepsilon_c - \varepsilon_0}{\varepsilon_r - \varepsilon_0} \times 100\% \tag{12}$$

where ε_c is the strain at the end of the creep phase at the corresponding stress level.

3.4.3 Linear amplitude sweep tests

In accordance with AASHTO T391-20, the damage accumulation in bitumen was calculated using Equation 13 (Kim et al., 2006):

$$D(t) \cong \sum_{i=1}^{N} \left[\pi I_D \gamma_0{}^2 \left(|G*|\sin\delta_{i-1} - |G*|\sin\delta_i\right)\right]^{\frac{\alpha}{1+\alpha}} \left(t_i - t_{i-1}\right)^{\frac{1}{1+\alpha}} \tag{13}$$

where $D(t)$ is the damage accumulation at time t, I_D is the initial complex modulus (G^*), and α is the rheological parameter determined from frequency sweep results.

The relationship between $|G^*|\sin\delta$ and $D(t)$ is expressed by Equation 14:

$$|G*|\sin\delta = C_0 - C_1(D)^{C_2} \tag{14}$$

where C_0 is the average $|G^*|\sin\delta$ at 0.1% strain, and C_1 and C_2 are curve-fitting coefficients derived from Equation 15 (Hintz et al., 2011).

$$\log\left(C_0 - |G*|\sin\delta\right) = \log\left(C_1\right) + C_2\log\left(D\right) \tag{15}$$

The fatigue failure of bitumen is defined as a 35% reduction in undamaged $|G^*|\sin\delta$, according to the latest AASHTO standard. The corresponding damage accumulation at failure (D^f) is determined by Equation 16.

$$D_f = \left(0.35\frac{C_0}{C_1}\right)^{\frac{1}{C_2}} \tag{16}$$

The parameters A and B are fitting coefficients used to estimate the fatigue life, as defined in Equations 17, 18:

$$A_{35} = \frac{f\left(D_f\right)^k}{k\left(\pi I_D C_1 C_2\right)^\alpha} \tag{17}$$

$$B = 2\alpha \tag{18}$$

The fatigue life (N_f) at any strain level (γ) of interest is calculated by Equation 19:

$$N_f = A_{35}(\gamma)^{-B} \tag{19}$$

3.4.4 Bending beam rheometer (BBR) tests

The stiffness (S) and creep rate (m-value) of bitumen were measured using BBR tests. Based on these results, the critical temperatures (T_c), where cracking is expected to occur due to low-temperature thermal stress, were determined using Equations 20, 21:

$$T_{C,S} = T_1 + \frac{(T_1 - T_2)(\log 300 - \log S_1)}{\log S_1 - \log S_2} - 10 \tag{20}$$

$$T_{C,m} = T_1 + \frac{(T_1 - T_2)(0.3 - m_1)}{m_1 - m_2} - 10 \tag{21}$$

where $T_{C,S}$ and $T_{C,m}$ represent the critical temperatures controlled by stiffness and m-value, respectively. S_1 and S_2 are stiffness values below and above 300 MPa, respectively; m_1 and m_2 are m-values above and below 0.3, respectively; and T_1 and T_2 are the corresponding test temperatures at which each criterion is met.

3.4.5 Fourier-transform infrared (FTIR) spectroscopy

The asymmetric stretching vibration at of the aliphatic structures 2,923 cm^{-1} was employed for normalisation. The absorbance value of this band was set to 1.0 and the complete spectrum was multiplied by a ratio factor. The tangent method was employed to quantify the areas of characteristic functional groups in the spectra, allowing the ageing fingerprints of bituminous binders to be tracked. For this method, the area under the tangent lines of the start of a specific peak and end of the corresponding peak was calculated (Hofko et al., 2017). Three key functional groups were selected to indicate ageing severity: carbonyl (1880–1,660 cm^{-1}, peak ≈1700 cm^{-1}), sulfoxide (1,079–984 cm^{-1}, peak ≈1,030 cm^{-1}), and the reference aliphatic band (1,525–1,350 cm^{-1}). The carbonyl index (CI) and sulfoxide index (SI) were calculated using Equations 22, 23, respectively.

$$CI = \frac{A_{1800-1660}}{A_{1525-1350}} \tag{22}$$

$$SI = \frac{A_{1079-984}}{A_{1525-1350}} \tag{23}$$

4 Results and discussion

4.1 High-temperature performance evaluation

The time-strain curves obtained from the MSCR tests of all bitumen samples are shown in Figure 1. As shown in Figure 1, the

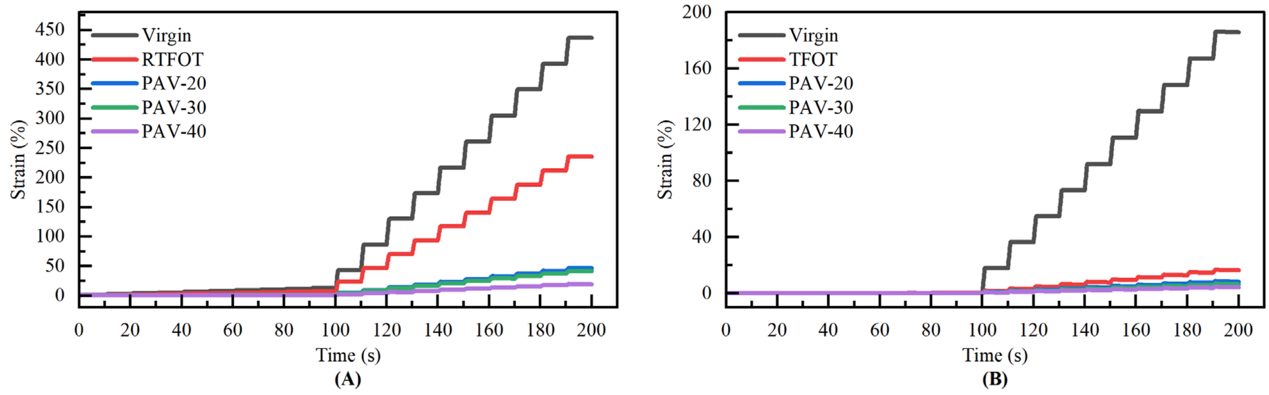

FIGURE 1
Strain accumulation curves: **(A)** Neat bitumen **(B)** CRMB.

incorporation of crumb rubber led to notable changes in the strain response of bituminous binders during the MSCR tests. A lower accumulation of strain indicates better resistance to permanent deformation, which is desirable for enhanced high-temperature performance. Clearly, adding crumb rubber substantially reduced the accumulated strain, confirming its beneficial effect on the high-temperature performance of bitumen.

At a relatively low stress level (0.1 kPa), neat (unmodified) bitumen exhibited a slight reduction in accumulated strain with increasing ageing severity. However, after the incorporation of crumb rubber, almost no difference was observed in the accumulated strain at 0.1 kPa, regardless of the ageing condition. This suggests that crumb rubber reduces the ageing sensitivity of bitumen. At the higher stress level (3.2 kPa), this effect became even more pronounced. Short-term ageing caused significant changes in the strain response of both neat bitumen and CRMB. For neat bitumen, the strain of the short-term aged binder fell between those of the virgin (unaged) and long-term aged binders. In contrast, the strain of the short-term aged CRMB was similar to that of the long-term aged CRMB. Furthermore, among the long-term aged binders, neat bitumen showed clear differences across ageing durations, whereas CRMB exhibited comparable strain values under different ageing levels. These results further confirm that crumb rubber reduces the ageing sensitivity of bitumen at high temperature, thereby enhancing its resistance to permanent deformation.

To further assess the influence of crumb rubber on high-temperature performance, the nonrecoverable compliance and recovery percentage were calculated, as shown in Figure 2. For comparison purposes, only the values measured at 3.2 kPa are presented here.

As shown in Figure 2, the incorporation of crumb rubber significantly reduced the nonrecoverable compliance of bitumen, indicating enhanced resistance to permanent deformation. The $J_{nr3.2}$ values of CRMB were 42.6%, 6.9%, 17.9%, 18.3%, and 21.5% of those of neat bitumen under virgin, short-term aged, and long-term aged conditions at 20, 30, and 40 h, respectively. The crumb rubber powder increased the stiffness of bitumen at high-temperature, thereby contributing to improved high-temperature performance.

It can also be observed from Figure 2 that the recovery percentages of CRMB under all ageing conditions were markedly higher than those of neat bitumen. Under virgin and short-term aged conditions, neat bitumen exhibited no recovery (zero recovery percentage). In contrast, CRMB displayed a recovery percentage of 0.5% in the virgin state, which increased substantially to 25.2% after short-term ageing. For both types of binders, the recovery percentage increased with ageing severity, indicating that ageing made the binders more elastic and recoverable after loading. Notably, the recovery percentages of CRMB were consistently higher than those of neat bitumen, averaging more than 15 times greater.

Ageing transforms bitumen from a viscoelastic to a more elastic state, resulting in higher stiffness and elasticity. Crumb rubber swells within the bitumen matrix, further increasing its stiffness and elasticity. The combined effects of crumb rubber modification and ageing enhance both the permanent deformation resistance and the recovery ability of bitumen at high temperatures (Si et al., 2024). Therefore, the incorporation of crumb rubber improves the rutting resistance of bitumen, and this improvement continues to take effect with ongoing ageing.

As mentioned earlier, the high-temperature performance was evaluated at stress levels of 0.1 kPa and 3.2 kPa. The difference between these two stress levels reflects the stress dependence of bituminous materials, as expressed in Equation 10. The corresponding results are presented in Figure 3.

As shown in Figure 3, the $J_{nr\text{-}diff}$ values of all CRMB samples were consistently higher than those of neat bitumen. In general, ageing did not alter the stress dependence of neat bitumen, as all binders exhibited similar $J_{nr\text{-}diff}$ values. However, for CRMB, ageing significantly affected the stress dependence of the binders, with the $J_{nr\text{-}diff}$ value of aged CRMB being nearly twice that of the unaged sample. It is noteworthy that ageing severity did not have a noticeable impact on stress dependence, as CRMB samples at all ageing levels exhibited comparable $J_{nr\text{-}diff}$ values. The results in Figure 3 indicate that although the incorporation of crumb rubber improved the high-temperature performance of bitumen, it slightly compromised the stress dependence, making the binder more sensitive to applied loading. Nevertheless, since the testing stress level of 3.2 kPa is sufficiently high to

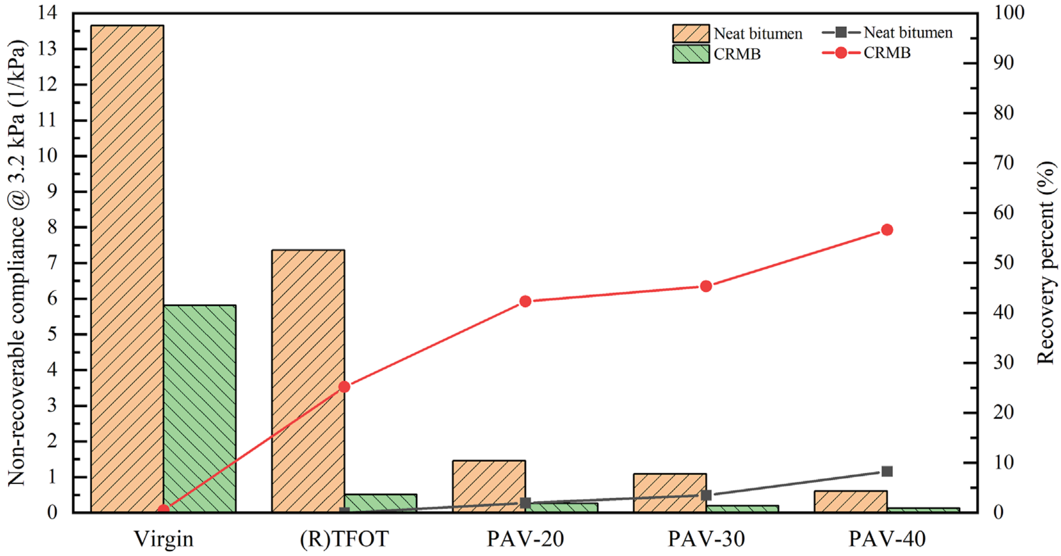

FIGURE 2
Nonrecoverable compliance and recovery percentage of bitumen.

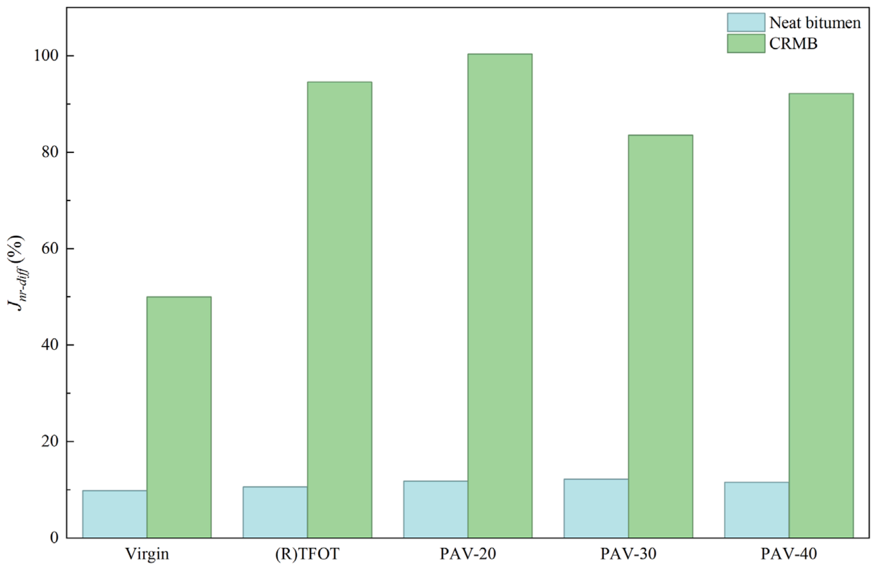

FIGURE 3
Differences in nonrecoverable compliance at two stress levels.

ensure that the binders can withstand heavy traffic loads, this slight increase in stress sensitivity does not necessarily affect the practical usability of CRMB. Overall, the high-temperature characterisation results suggest that the incorporation of crumb rubber can significantly enhance the rutting resistance of bitumen, regardless of the degree of ageing. This improvement became more pronounced with progressively severe ageing. Although the stress dependence was slightly compromised at all ageing levels, this effect does not hinder the application of CRMB in pavement engineering.

4.2 Low-temperature performance characterisation

Conventionally, stiffness and m-value are analysed as key indicators of the low-temperature performance of bitumen, particularly for determining its performance grade (PG). However, the PG classification is relatively broad, with an interval of 6 °C between grades, which limits its ability to accurately distinguish low-temperature performance. To address this limitation, the concept of critical temperature is introduced, representing the temperature at which bitumen is expected to experience thermal cracking. As

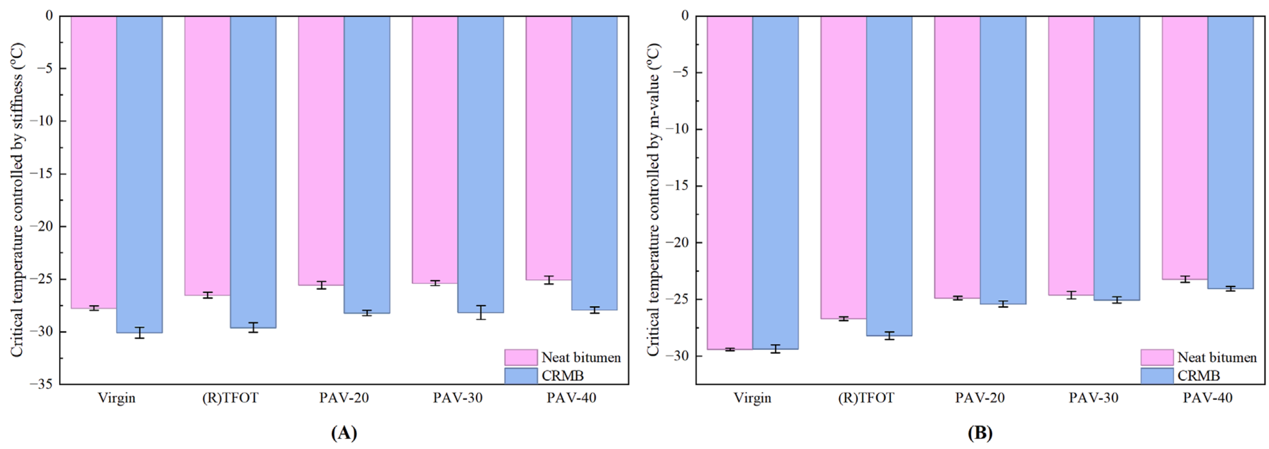

FIGURE 4
Critical temperatures for bituminous binders: **(A)** $T_{C,S}$ **(B)** $T_{C,m}$.

BBR tests provide both stiffness and m-value, two corresponding critical temperatures are determined for each sample: the critical temperature controlled by stiffness ($T_{C,S}$) and that controlled by m-value ($T_{C,m}$). The results are presented in Figure 4.

As shown in Figure 4, CRMB consistently exhibited lower critical temperatures controlled by stiffness (i.e., more negative values) than neat bitumen across all ageing conditions. This indicates that CRMB, even after ageing, retains superior flexibility and ductility at low temperatures compared with neat bitumen, which is advantageous for preventing thermal cracking in cold climates. Bitumen is highly temperature-sensitive: at low temperatures, its stiffness increases significantly, making it brittle and prone to cracking. The incorporation of crumb rubber reduced this temperature sensitivity, resulting in lower stiffness at low temperatures. Consequently, the brittleness of bitumen decreased, and the critical temperature controlled by stiffness was correspondingly reduced. Ageing resulted in a noticeable effect on both neat bitumen and CRMB. Both binders exhibited a general trend of decreasing flexibility (less negative $T_{C,S}$) as ageing became more severe. However, CRMB demonstrated a less pronounced shift in $T_{C,S}$ compared with neat bitumen, particularly under the severer ageing conditions (PAV-30 and PAV-40). The finding suggests that the incorporation of crumb rubber helped preserve the low-temperature performance of binders during ageing, rendering CRMB more resistant to the adverse effects of ageing in terms of low-temperature behaviour.

A similar trend was observed for the critical temperature controlled by m-value ($T_{C,m}$). The $T_{C,m}$ values of CRMB were consistently lower than those of neat bitumen at all ageing levels. At low temperatures, bitumen typically loses flexibility and ductility, leading to a reduced creep rate. The incorporation of crumb rubber enhanced the elasticity of bitumen, allowing it to sustain creep even at low temperatures. This improvement increased the recoverability of bitumen after loading and reduced the risk of cracking due to insufficient creep capacity. Moreover, the $T_{C,m}$ of neat bitumen decreased sharply with ageing severity, whereas CRMB exhibited a slower rate of reduction, indicating better ageing resistance.

TABLE 1 ΔT_C for different bitumen.

Ageing conditions	ΔT_C (°C)	
	Neat bitumen	CRMB
Virgin	1.62	−0.73
Short-term aged	0.17	−1.42
PAV-20	−0.67	−2.82
PAV-30	−0.76	−3.11
PAV-40	−1.85	−3.86

The difference between the critical temperatures controlled by stiffness and m-value is defined as ΔT_C, which is also related to the cracking resistance of bitumen. The ΔT_C values for the different binders are presented in Table 1. As shown in Table 1, the values of ΔT_C for different binders varied significantly. According to the definition of ΔT_C, a positive value indicates that thermal cracking behaviour is controlled by stiffness, meaning brittleness is the dominant cause of cracking. In contrast, a negative value suggests that cracking is primarily controlled by the m-value, implying that the loss of creep ability governs the cracking behaviour. As shown in Table 1, for neat bitumen, the virgin and short-term aged binders were stiffness-controlled, whereas all long-term aged binders were m-value-controlled. However, for CRMB, all binders, regardless of ageing condition, were m-value-controlled. This observation indicates that the incorporation of crumb rubber altered the thermal cracking mechanism of bitumen. Moreover, under the same ageing conditions, the ΔT_C values of neat bitumen were consistently higher than those of CRMB.

Previous studies have reported that more negative ΔT_C values correspond to a higher cracking potential (Hu et al., 2024a). Based solely on this criterion, CRMB would appear to have poorer cracking resistance than neat bitumen, which seems inconsistent with the results obtained from the critical temperature analysis. However, it is important to note that the incorporation of crumb rubber significantly lowered the critical temperatures, indicating that the modified bitumen can withstand lower temperatures before cracking occurs. According to the Asphalt Institute, most Departments of Transportation (DoTs) in the United States have adopted a ΔT_C threshold of −5 °C after 40 h of PAV ageing (Asphalt Institute Technical Advisory Committee, 2019). Therefore, as long as the ΔT_C value remains above −5 °C at the PAV-40 condition, the binder is considered suitable for pavement applications. Based on this criterion, the CRMB used in this study satisfied the requirement, confirming its suitability for practical use.

4.3 Fatigue performance evaluation

The fatigue performance of the binders was evaluated using the linear amplitude sweep (LAS) test. Since the fatigue life of bituminous materials is highly dependent on the applied loading level (i.e., stress or strain), six strain levels, 2.5%, 5%, 7.5%, 10%, 12.5%, and 15% respectively, were selected in this study to calculate the fatigue life of the binders. The results are presented in Figure 5. As shown in Figure 5, the fatigue life of bituminous binders was highly dependent on strain for both neat bitumen and CRMB. The fatigue life decreased almost linearly with increasing strain when plotted on a double logarithmic scale. For neat bitumen, at relatively low strain levels, ageing exhibited a beneficial effect on fatigue life, primarily due to the increased stiffness (Chen and Bahia, 2021). Consequently, with progressively higher ageing severity, the fatigue life of neat bitumen increased. However, as the applied strain increased, the ranking of fatigue life among binders with different ageing levels changed markedly. At moderate strain levels (approximately 10%–12.5%), no consistent trend was observed between ageing severity and fatigue life. When the applied strain was very high (e.g., 15%), fatigue life decreased sharply with ageing severity. Under such conditions, fracture damage dominated over fatigue damage because the bitumen became stiffer and more brittle (Hu et al., 2024c). For CRMB, the trend differed considerably. Across all ageing levels the fatigue life of aged binders was consistently lower than that of the virgin binder. This finding indicates that the incorporation of crumb rubber altered the fatigue damage mechanism of bitumen. Moreover, the fatigue lives of all aged CRMB samples were quite similar, suggesting that modification had a more pronounced influence on fatigue performance than ageing. It was also observed that the fatigue life of CRMB was significantly lower than that of neat bitumen, implying that the addition of crumb rubber adversely affected the fatigue resistance of the binder.

The roles of parameters A and B will be further analysed, as shown in Figure 6.

It is also evident from Figure 6 that parameter A values for CRMB were consistently lower than those for neat bitumen, while parameter B values were consistently higher. These two effects collectively contributed to the reduced fatigue life of CRMB compared to neat bitumen. Furthermore, ageing enhanced the strain dependency of fatigue behaviour for all binders. The incorporation of crumb rubber exhibited a similar trend, further deteriorating the fatigue performance of CRMB.

4.4 Comprehensive evaluation of the rheological properties of bitumen

The master curves were constructed to illustrate the overall rheological performance of the bitumen during the ageing process, with the reference temperature being 25 °C, as presented in Figure 7.

As shown in Figure 7, the variations in complex modulus were straightforward. Generally, for all types of bitumen, the complex modulus increased almost linearly with decreasing frequency on the double-logarithmic scale. Moreover, ageing led to a more pronounced influence on the low-temperature (high-frequency) performance of bitumen, as the master curves in the high-frequency region tended to bend and converge. This indicates that at very low temperatures, bitumen behaves like a glassy material, with the complex modulus approaching the glassy modulus (approximately 100 MPa to 1 GPa) (Di Benedetto et al., 2004). This trend was observed for both bitumens.

Additionally, the complex modulus of CRMB was higher than that of neat bitumen under the same ageing condition at low-frequency range. This finding agrees with the observation that the incorporation of CRMB increased the rutting resistance of bitumen, as reported in the MSCR subsection. The master curves also revealed that the complex modulus of neat bitumen gradually increased with ageing, whereas for CRMB, the difference between virgin and aged binders was more evident, while differences among various ageing levels were relatively small. This suggests that crumb rubber has the potential to improve long-term ageing resistance. Regarding the phase angle, the master curves of neat bitumen and CRMB exhibited distinct patterns. For neat bitumen, the phase angle curves of virgin and short-term aged binders showed a single-peak parabolic shape, whereas those of long-term aged binders decreased almost linearly with decreasing frequency. Ageing gradually reduced the phase angle with increasing ageing severity, leading to a more elastic response and consequently better recoverability after loading, consistent with the MSCR results.

For CRMB, the phase angle master curves at all ageing levels displayed a plateau in the low-frequency range, followed by a gradual decrease with increasing reduced frequency, suggesting the nonlinearity of this material. These results indicate that at high temperatures, the viscoelastic properties of CRMB changed more slowly, implying better temperature stability, which again aligns with the MSCR findings. Moreover, the phase angles of CRMB at high-temperature ranges were consistently higher than those of neat bitumen, suggesting a more viscous response. To further analyse the viscoelastic behaviour of bitumen in relation to crumb rubber modification and ageing, a black space diagram was plotted with the integrated G–R parameter, as shown in Figure 8.

As shown in Figure 8, ageing shifted the data points from the bottom right to the top left, indicating that the binders became stiffer and more elastic. This trend was observed for both neat bitumen and CRMB. In the black space diagram, the scatter points of neat bitumen moved progressively with ageing, whereas for CRMB, the virgin binder was far from the aged points, which were closely clustered. This provides strong evidence that the incorporation of crumb rubber altered the ageing pathway of bitumen. The integrated G–R parameter has two critical thresholds. A value of 180 kPa corresponds to the cracking warning threshold. Binders with G–R values below this threshold are considered in

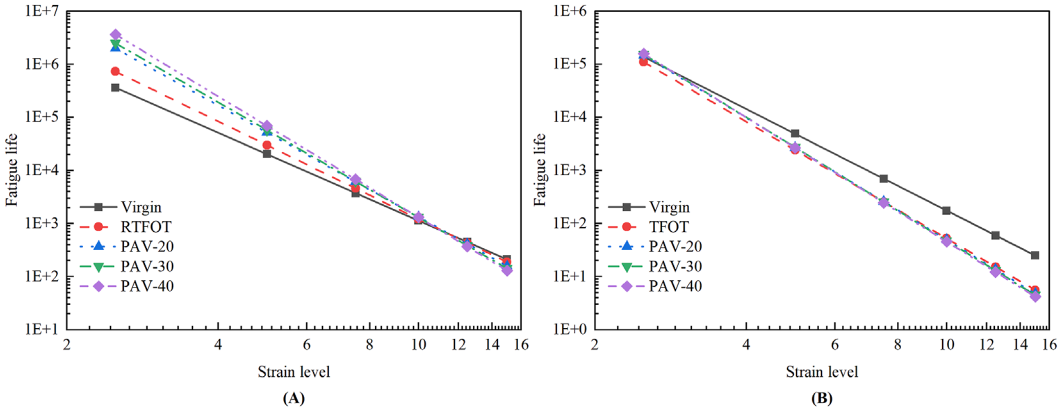

FIGURE 5
Fatigue life of bitumen at varying ageing conditions: **(A)** Neat bitumen **(B)** CRMB.

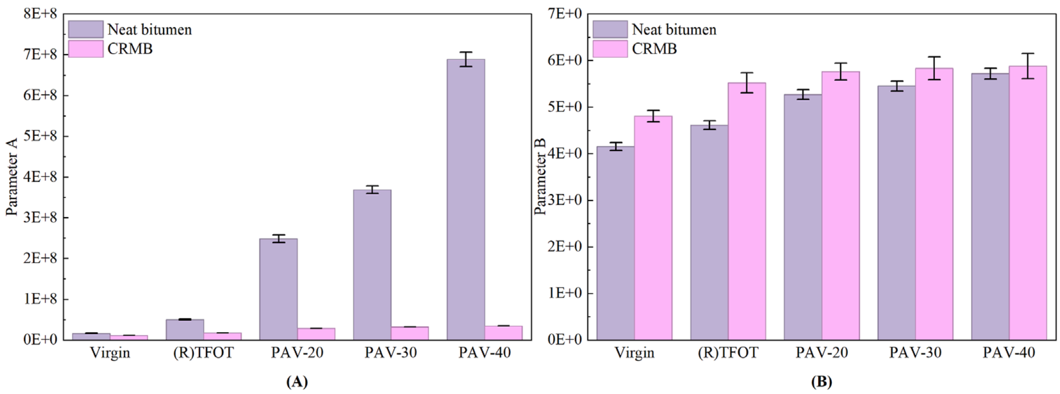

FIGURE 6
Fatigue life determining parameters: **(A)** Parameter A **(B)** Parameter B.

the safe zone, with minimal risk of cracking. When the G–R parameter lies between 180 kPa and 600 kPa, the binder is at risk of cracking, and microcracks may develop and propagate. Values exceeding 600 kPa indicate a high likelihood of significant cracking (Airey et al., 2022). Based on Figure 8, all neat bitumen data points remained in the safe zone, even after 40 h of PAV ageing, indicating satisfactory durability. In contrast, for CRMB, the G–R parameter approached the cracking warning threshold after 30 h of PAV ageing and exceeded it after 40 h, suggesting a potential risk of microcrack formation. However, this risk was not critical, as the 40-h PAV-aged CRMB exhibited a G–R value of 213 kPa, only slightly above the warning limit.

To further support the engineering applicability of CRMB, the performance grades (PG) of both neat bitumen and CRMB were determined. The PG for both neat bitumen and CRMB was PG70-22, suggesting that CRMB has comparable performance grade with the corresponding base bitumen. Moreover, the continuous PG for neat bitumen was PG 71.8-25.2 while that for CRMB was PG 74.5-26.8, suggesting that CRMB could be adopted in slightly hotter regions as well as slightly colder regions, further endorsed for the engineering feasibility of CRMB.

4.5 Chemical properties of bituminous binders during ageing process

FTIR spectroscopy was employed to evaluate the chemical changes occurring in both neat bitumen and CRMB under all ageing conditions. The corresponding spectra are presented in Figure 9.

As shown in Figure 9, the spectra of neat bitumen and CRMB were similar, indicating that the interaction between crumb rubber and bitumen was primarily physical swelling, with no evident chemical reactions. It is noteworthy that no peaks were observed at 965 cm^{-1}, corresponding to the = C–H out-of-plane vibration typical of rubber, because the ATR mode can only detect a thin film of approximately 2 μm, rendering the crumb rubber particles undetectable. After ageing, both neat bitumen and CRMB exhibited increased intensities in ketones (mainly carbonyls) and sulfoxides. The quantified carbonyl index and sulfoxide index are presented in Figure 10.

Figure 10 shows that the carbonyl indices of both neat bitumen and CRMB increased continuously with ageing due to oxidation. The carbonyl values for neat bitumen and CRMB were nearly identical, indicating that the incorporation of crumb rubber

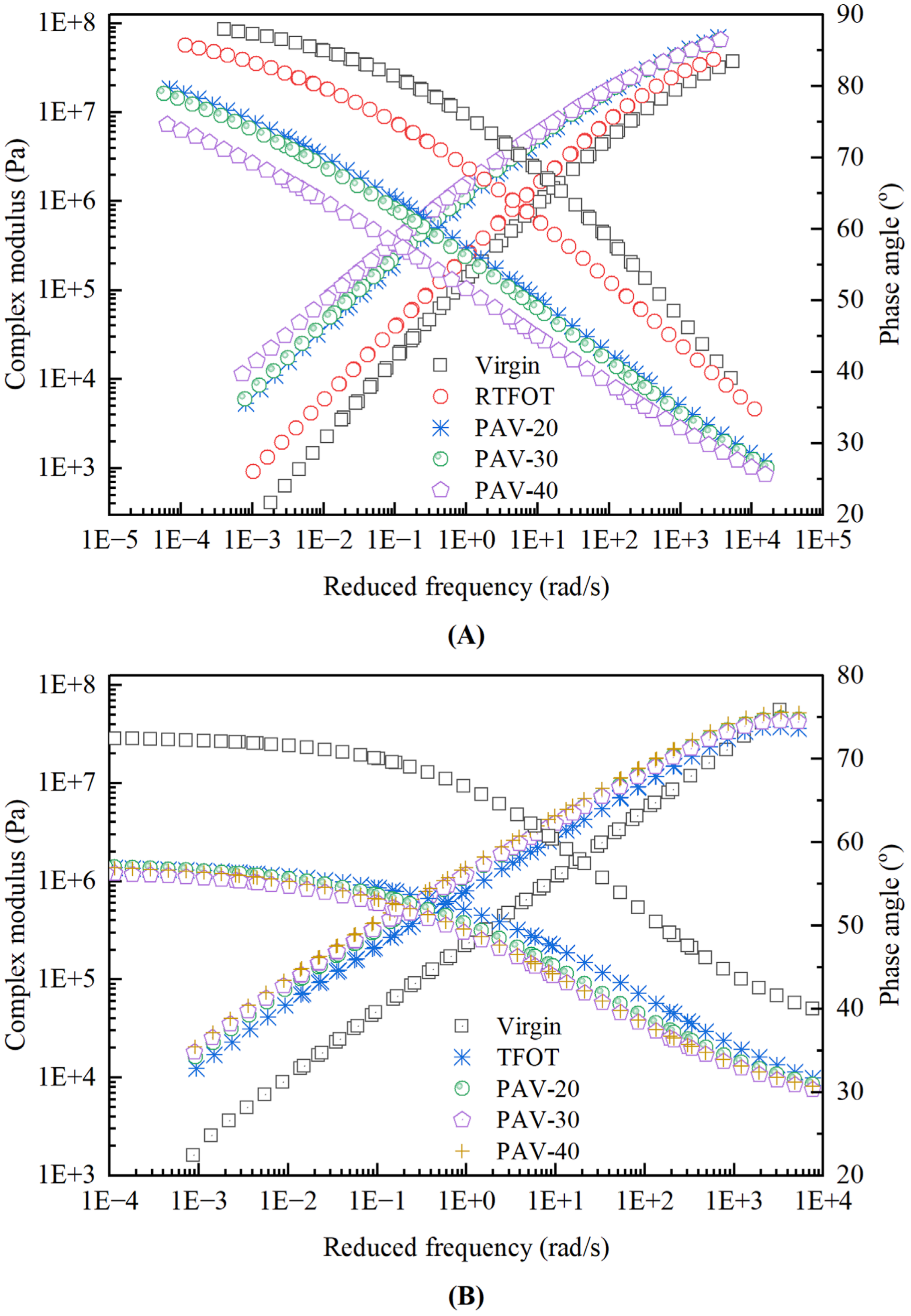

FIGURE 7
Master curves for complex modulus and phase angle: **(A)** Neat bitumen **(B)** CRMB.

did not alter the chemical ageing mechanism of bitumen. In contrast, the sulfoxide index of neat bitumen initially increased and then decreased. This behaviour arises because the formation and decomposition of sulfoxides occur simultaneously during ageing (Hu et al., 2025a; Hu et al., 2024b). At the early stage of oxidation, sulfoxide formation dominates, leading to an increase in

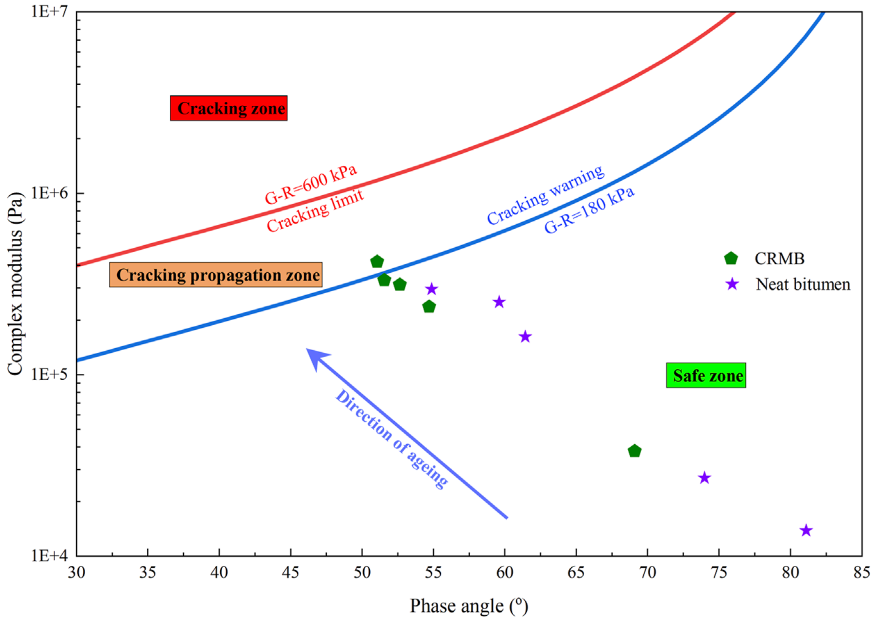

FIGURE 8
Black space diagram with G-R parameter.

the sulfoxide index. As ageing progresses, decomposition becomes more significant, causing the sulfoxide index to decline. For CRMB, which contains sulphur from the crumb rubber, oxidation of sulphur occurs alongside bitumen oxidation, resulting in a continuous increase in the sulfoxide index. Overall, the incorporation of crumb rubber did not substantially alter the chemical oxidation pathway of bitumen. CRMB exhibited comparable ageing resistance to neat bitumen, demonstrating its chemical stability and suitability as a partial bitumen substitute to support sustainable pavement development.

The differences arise because the mechanical ageing sensitivity observed in rheological tests is controlled not only by chemical oxidation but also by rubber swelling, particle elasticity, and changes in the maltene-asphaltene balance induced by CRMB modification. FTIR detects only chemical functional group evolution near the surface, whereas the rubber particles are distributed within the binder matrix and cannot be detected in ATR mode due to its shallow penetration depth. As a result, FTIR may not fully capture the mechanisms that govern ageing sensitivity in CRMB. Although CRMB undergoes chemical oxidation similar to neat bitumen, its rheological response is partially insulated by the contribution of the swollen rubber network, which reduces mechanical hardening during ageing. This reconciles the FTIR and rheological findings.

4.6 Statistical analysis

To evaluate the significance of the results, a statistical analysis was conducted. The two-factors analysis of variance (AVOVA) of nonrecoverable compliance is shown in Table 2.

As shown in Table 2, two-factor ANOVA results indicate that neither the binder type nor the ageing level significantly affected the nonrecoverable compliance J_{nr} at the 0.05 level (binder type: F = 4.64, p = 0.098; ageing level: F = 4.92, p = 0.076). However, the ageing level showed a trend toward significance, suggesting that long-term oxidation may increase susceptibility to nonrecoverable compliance. The binder type effect was comparatively weaker, indicating that the incorporation of crumb rubber into bitumen has a slight improvement impact on the rutting resistance of bitumen but this effect is statistically insignificant.

The two-factors analysis of variance (AVOVA) of ΔT_c is shown in Table 3.

Two-way ANOVA revealed statistically significant effects of both binder type (F = 221.06, p < 0.001) and ageing level (F = 65.90, p < 0.001) on ΔT_c, as shown in Table 3. This indicates that ageing-induced low-temperature embrittlement is strongly dependent on the binder composition and oxidation degree. The neat bitumen retained more favourable ΔT_c, values compared to the CRMB, across all ageing stages, suggesting reduced resistance to thermo-oxidative cracking, which needs to be monitored during service life though its value met the requirements for current specifications.

The two-factors analysis of variance (AVOVA) of fatigue life at 15% strain measured by linear amplitude sweep is shown in Table 4.

The two-way ANOVA results for fatigue life at 15% strain, as shown in Table 4, demonstrating that binder type had a statistically significant effect on fatigue resistance (F = 170.76, p < 0.001), with neat bitumen consistently achieving higher N_f values than the CRMB. In contrast, ageing level did not exhibit a statistically significant influence (F = 2.33, p = 0.217), indicating that at large strain amplitudes, the fatigue response is dominated by the inherent binder modification rather than oxidative embrittlement. However, the statistical insignificant is attributed to the high ageing resistance of CRMB.

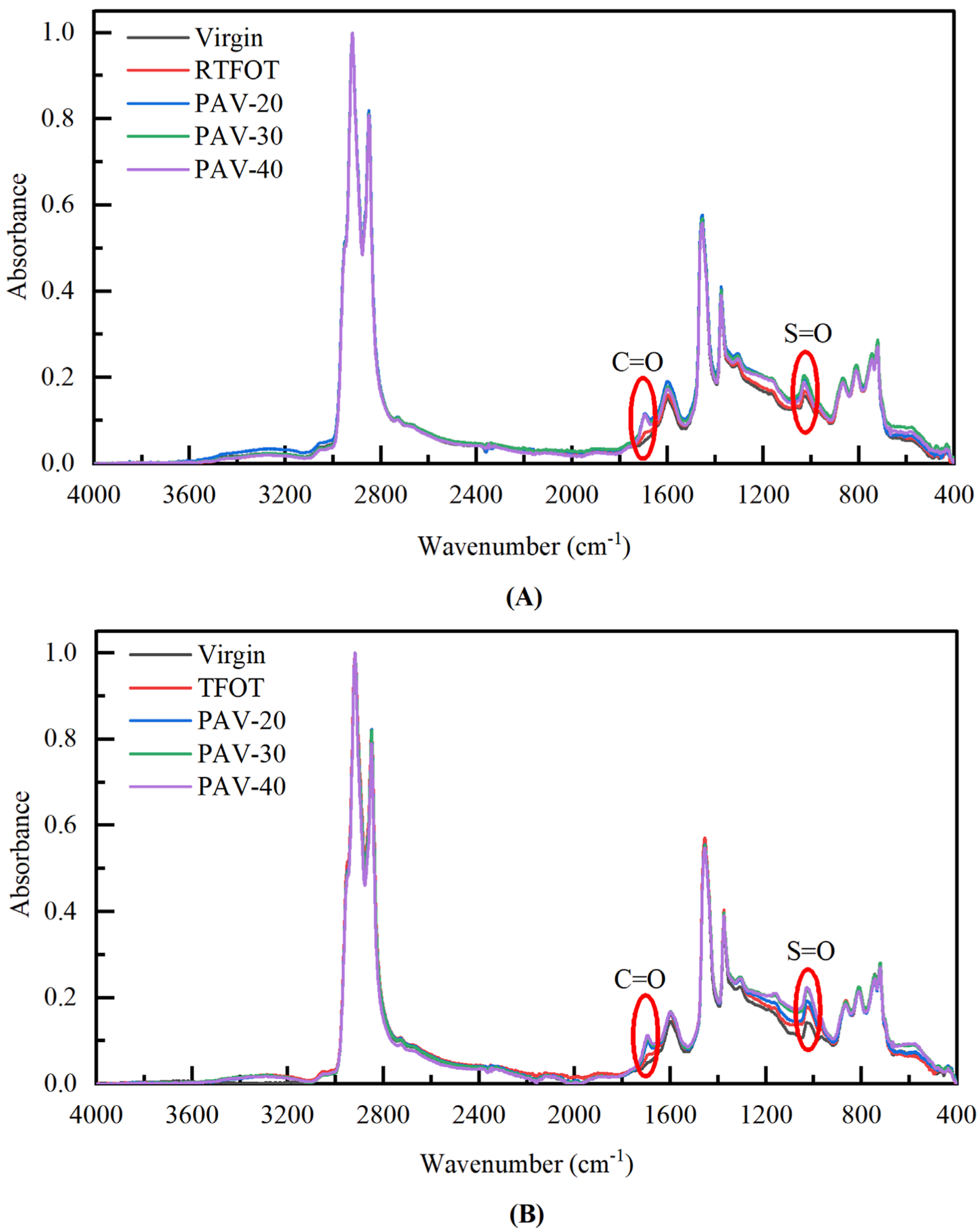

FIGURE 9
FTIR spectra for bitumen: **(A)** Neat bitumen **(B)** CRMB.

Finally, the two-factors analysis of variance (AVOVA) of carbonyl index is shown in Table 5.

As shown in Table 5, the two-way ANOVA results demonstrated that the carbonyl index was significantly affected by the ageing level ($F = 272.14$, $p < 0.001$), confirming that oxidative ageing strongly increases carbonyl formation. In contrast, the binder type did not show a statistically significant influence ($F = 1.08$, $p = 0.357$), indicating that the overall carbonyl generation kinetics of CRMB and neat binders are similar. These findings imply that FTIR carbonyl evolution is primarily governed by thermo-oxidative exposure rather than polymer modification. This suggests that FTIR oxidation markers alone may not represent the reduced ageing sensitivity of CRMB due to the rubber network's physical hardening and non-linear recoverability mechanisms, which are better captured by rheological indicators such as ΔT_c and MSCR parameters.

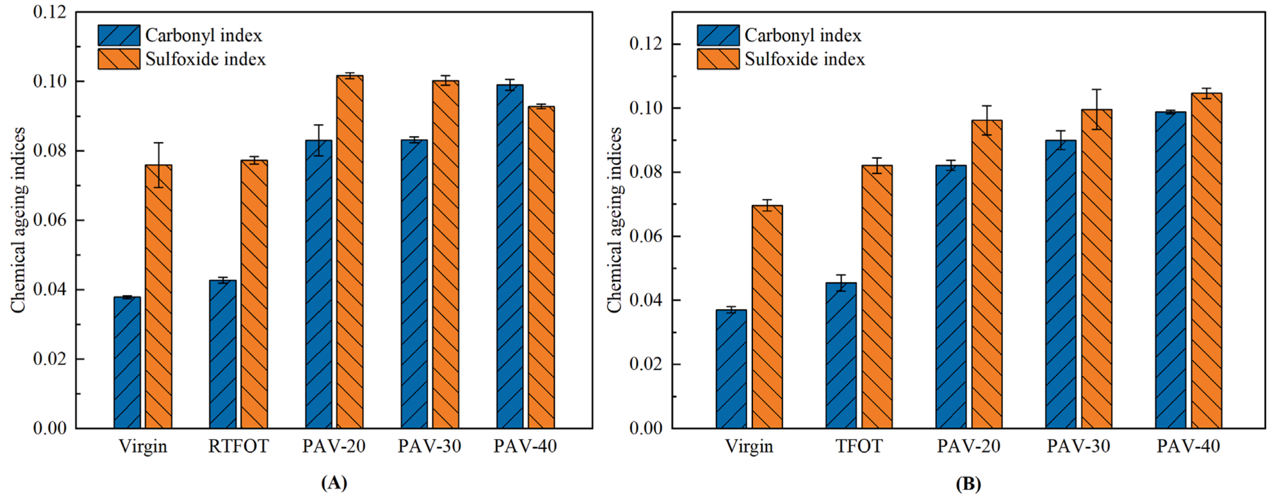

FIGURE 10
Chemical ageing indices based on carbonyl index and sulfoxide index: **(A)** Neat bitumen **(B)** CRMB.

TABLE 2 Two-factor ANOVA of nonrecoverable compliance.

Source of variation	*SS*	*df*	*MS*	*F*	*P-value*	*F crit*
Bitumen type	29.74935	1	29.74935	4.637682	0.097595	7.708647
Ageing situation	126.3544	4	31.5886	4.924406	0.075855	6.388233
Error	25.65881	4	6.414703			
Total	181.7626	9				

TABLE 3 Two-factor ANOVA of ΔTc.

Source of variation	*SS*	*df*	*MS*	*F*	*P-value*	*F crit*
Bitumen type	10.92025	1	10.92025	221.0577	0.000119	7.708647
Ageing situation	13.02136	4	3.25534	65.89757	0.000664	6.388233
Error	0.1976	4	0.0494			
Total	24.13921	9				

TABLE 4 Two-factor ANOVA of fatigue life at 15% strain.

Source of variation	*SS*	*df*	*MS*	*F*	*P-value*	*F crit*
Bitumen type	61,598.12	1	61,598.12	170.7611	0.000198	7.708647
Ageing situation	3,356.204	4	839.051	2.326001	0.216834	6.388233
Error	1,442.907	4	360.7269			
Total	66,397.24	9				

TABLE 5 Two-factor ANOVA of carbonyl index.

Source of variation	SS	df	MS	F	P-value	F crit
Bitumen type	5.96E-06	1	5.96E-06	1.080569	0.357274	7.708647
Ageing situation	0.006004	4	0.001501	272.1364	4.01E-05	6.388233
Error	2.21E-05	4	5.52E-06			
Total	0.006032	9				

5 Conclusion

This study evaluated the performance of crumb rubber modified bitumen (CRMB) after long-term ageing to assess its durability and potential for enhancing sustainability in the pavement sector. Systematic physicochemical properties were examined using rheological and chemical characterisation methods. Based on the results, the following conclusions can be drawn:

1. Crumb rubber significantly improved the permanent deformation resistance and elastic recoverability of bitumen at high temperatures. This effect became more pronounced after ageing.
2. Crumb rubber reduced the stiffness and enhanced the creep properties of bitumen at low temperatures, resulting in lower critical temperatures after different durations of long-term ageing.
3. Although ΔT_c was slightly reduced with the addition of crumb rubber, it remained within current specification limits.
4. The fatigue life of CRMB was lower than that of neat bitumen. Future studies could explore activation or treatment of crumb rubber to enhance fatigue performance. The durability, as indicated by the G–R parameter, was slightly weakened but remained within acceptable limits.
5. The incorporation of crumb rubber did not alter the chemical properties of bitumen. CRMB exhibited comparable ageing resistance to neat bitumen in terms of functional group evolution.
6. ANOVA confirmed that CRMB offers statistically significant advantages and disadvantages in rheological performance while chemical oxidation indices change similarly to neat binders, highlighting the mechanical resilience contributed by the rubber network.

Data availability statement

The original contributions presented in the study are included in the article/supplementary material, further inquiries can be directed to the corresponding author.

Author contributions

JL: Conceptualization, Writing – original draft, Funding acquisition, Investigation, Methodology, Formal Analysis, Project administration, Data curation. QY: Writing – original draft, Methodology, Investigation, Supervision, Project administration, Resources, Formal Analysis. YZ: Supervision, Writing – original draft, Investigation, Formal Analysis, Methodology. SW: Writing – original draft, Formal Analysis, Investigation. WW: Formal Analysis, Investigation, Writing – original draft. WS: Supervision, Writing – review and editing, Investigation. RW: Supervision, Writing – review and editing, Investigation.

Funding

The author(s) declared that financial support was received for this work and/or its publication. This research was funded by the Scientific Research Project of Shaanxi Polytechnic University under the grant number of 2024YKYB-022.

Conflict of interest

The author(s) declared that this work was conducted in the absence of any commercial or financial relationships that could be construed as a potential conflict of interest.

Generative AI statement

The author(s) declared that generative AI was not used in the creation of this manuscript.

Any alternative text (alt text) provided alongside figures in this article has been generated by Frontiers with the support of artificial intelligence and reasonable efforts have been made to ensure accuracy, including review by the authors wherever possible. If you identify any issues, please contact us.

Publisher's note

References

AASHTO (2020). *Estimating fatigue resistance of asphalt binders using the linear amplitude sweep*. Washington D.C.: American Association of State Highway and Transportation Officials.

Airey, G. D., Rowe, G. M., Sias, J. E., Di Benedetto, H., Sauzeat, C., and Dave, E. V. (2022). Black space rheological assessment of asphalt material behavior. *J. Test. Eval.* 50, 770–787. doi:10.1520/jte20210205

Asphalt Institute Technical Advisory Committee (2019). State-of-the-Knowledge: use of the Delta Tc parameter to characterize asphalt binder behavior.

ASTM (2022). *Standard test method for effect of heat and air on a moving film of asphalt binder (rolling thin-film oven test)*. West Conshohocken, PA: ASTM International.

ASTM (2024). *Standard test method for multiple stress creep and recovery (MSCR) of asphalt binder using a dynamic shear rheometer*. West Conshohocken, PA: ASTM International.

ASTM (2025). *Standard test method for determining the flexural creep stiffness of asphalt binder using the bending beam rheometer (BBR)*. West Conshohocken, PA: ASTM International.

Cannone Falchetto, A., Yin, F., Cavalli, M. C., Mangiafico, S., Biligiri, K. P., Cantot, J., et al. (2025). On the new RILEM technical committee TC APD: alternative paving materials – design and performance. *RILEM Tech. Lett.* 9, 68–75. doi:10.21809/rilemtechlett.2024.196

Chen, H., and Bahia, H. U. (2021). Modelling effects of aging on asphalt binder fatigue using complex modulus and the LAS test. *Int. J. Fatigue* 146, 106150. doi:10.1016/j.ijfatigue.2021.106150

Di Benedetto, H., Olard, F., Sauzéat, C., and Delaporte, B. (2004). Linear viscoelastic behaviour of bituminous materials: from binders to mixes. *Road Mater. Pavement Des.* 5, 163–202. doi:10.1080/14680629.2004.9689992

EAPA (2025). Asphalt in figures 2023. Brussels: European asphalt pavement association.

Espinosa, L. V., Vasconcelos, K., Alvarez, A. E., Bhasin, A., and Bernucci, L. (2024). Moisture damage susceptibility of a wood-based bio-binder for total replacement of asphalt binders. *Road Mater. Pavement Des.* 25, 45–55. doi:10.1080/14680629.2023.2191728

Gao, Y., Zhang, Y., Omairey, E. L., Al-Malaika, S., and Sheena, H. (2021). Influence of anti-ageing compounds on rheological properties of bitumen. *J. Clean. Prod.* 318, 128559. doi:10.1016/j.jclepro.2021.128559

GDoT (2025). *Asphalt cement price index*. Georgia, Georgia Department of Transportation.

Hintz, C., Velasquez, R., Johnson, C., and Bahia, H. (2011). Modification and validation of linear amplitude sweep test for binder fatigue specification. *Transp. Res. Rec.* 2207, 99–106. doi:10.3141/2207-13

Hofko, B., Alavi, M. Z., Grothe, H., Jones, D., and Harvey, J. (2017). Repeatability and sensitivity of FTIR ATR spectral analysis methods for bituminous binders. *Mater. Struct.* 50, 187. doi:10.1617/s11527-017-1059-x

Hu, Y., Allanson, M., Sreeram, A., Ryan, J., Wang, H., Zhou, L., et al. (2024a). Characterisation of bitumen through multiple ageing-rejuvenation cycles. *Int. J. Pavement Eng.* 25, 2365350. doi:10.1080/10298436.2024.2365350

Hu, Y., Ryan, J., Sreeram, A., Allanson, M., Pasandín, A. R., Zhou, L., et al. (2024b). Optimising the dosage of bio-rejuvenators in asphalt recycling: a rejuvenation index based approach. *Constr. Build. Mater.* 433, 136761. doi:10.1016/j.conbuildmat.2024.136761

Hu, Y., Sreeram, A., Bahia, H. U., Airey, G. D., Si, W., Li, B., et al. (2024c). Assessing correlations between two linear amplitude sweep (LAS) standards for evaluating the fatigue properties of aged bitumen. *Int. J. Pavement Eng.* 25, 2375419. doi:10.1080/10298436.2024.2375419

Hu, Y., Wang, H., Zhou, L., and Airey, G. D. (2024d). "Towards an enhanced understanding of the functional groups within bitumen during ageing processes," in *Advances in functional pavements*. CRC Press.

Hu, Y., Cheng, X., Sreeram, A., Si, W., Li, B., Pipintakos, G., et al. (2025a). Enhancing fatigue resistance and low-temperature performance of asphalt pavements using antioxidant additives. *Mater. Struct.* 58, 46. doi:10.1617/s11527-025-02574-4

Hu, Y., Hejazi, S., Patel, D., Jahan, H., Özdemir, D. K., Yin, Y., et al. (2025b). Comprehensive characterisation of lignin-based bio-bitumen as a sustainable paving material. *Constr. Build. Mater.* 502, 144455. doi:10.1016/j.conbuildmat.2025.144455

Hu, Y., Sreeram, A., Al-Tabbaa, A., and Airey, G. D. (2025c). Physicochemical compatibility assessment of bio-additives and bitumen using solubility science-based approaches. *Fuel* 387, 134361. doi:10.1016/j.fuel.2025.134361

Hu, Y., Yin, Y., Sreeram, A., Liu, J., Si, W., Tang, D., et al. (2025d). Nano-aggregation of asphaltenes and its influence on the multiscale properties of bitumen recycled through multiple ageing and rejuvenation cycles. *Chem. Eng. J.* 512, 162348. doi:10.1016/j.cej.2025.162348

Hu, Y., Yin, Y., Sreeram, A., Si, W., Airey, G. D., Li, B., et al. (2025e). Atomic force microscopy (AFM) based microstructural and micromechanical analysis of bitumen during ageing and rejuvenation. *Constr. Build. Mater.* 467, 140387. doi:10.1016/j.conbuildmat.2025.140387

Kim, Y. R., Lee, H. J., Little, D. N., and Kim, Y. R. (2006). A simple testing method to evaluate fatigue fracture and damage performance of asphalt mixtures (with discussion).

Kumar, A., Choudhary, R., Kandhal, P. S., Julaganti, A., Behera, O. P., Singh, A., et al. (2020). Fatigue characterisation of modified asphalt binders containing warm mix asphalt additives. *Road Mater. Pavement Des.* 21, 519–541. doi:10.1080/14680629.2018.1507921

Li, B., Zhao, H., Zhou, J., Yao, T., Guo, F., and Hu, Y. (2024). Investigation on sound absorption coefficients of porous asphalt concrete under different clogging conditions. *Constr. Build. Mater.* 428, 136081. doi:10.1016/j.conbuildmat.2024.136081

Lo Presti, D., Izquierdo, M. A., and Jiménez Del Barco Carrión, A. (2018). Towards storage-stable high-content recycled tyre rubber modified bitumen. *Constr. Build. Mater.* 172, 106–111. doi:10.1016/j.conbuildmat.2018.03.226

MAA (2024). *Prevailing monthly price for asphalt*. Glen Burnie: Maryland asphalt association. Available online at: https://mdasphalt.org/asphalt-index/(Accessed June 14, 2024).

Mirwald, J., Khalighi, S., Varveri, A., Hofko, B., Adwani, D., Cannone-Falchetto, A., et al. (2025). Evaluating the reproducibility and consistency of different sample preparation techniques used for ATR-FTIR spectroscopy from the RILEM 295-FBB TG1 round robin test. *Mater. Struct.* 58, 255. doi:10.1617/s11527-025-02755-1

NAPA (2020). *The asphalt pavement industry fast facts*. Greenbelt, MD: National asphalt pavement association.

Patel, D., Jahan, H., Hu, Y., Hejazi, S., Roja, K. L., Airey, G., et al. (2025). Incorporating bio-based lignin as a sustainable fine aggregate in asphalt mixtures: comprehensive analysis of long-term performance. *Sustain. Mater. Technol.* 46, e01734. doi:10.1016/j.susmat.2025.e01734

Shi, K., Ma, F., Fu, Z., Song, R., Yuan, D., and Ogbon, A. W. (2024). Enhancing aged SBS-Modified bitumen performance with unaged bitumen additives. *Constr. Build. Mater.* 412, 134768. doi:10.1016/j.conbuildmat.2023.134768

Shi, K., Ma, F., Falchetto, A. C., Fu, Z., Yuan, D., Song, R., et al. (2025). Comprehensive review on the composition, influence, and inhibition of asphalt fumes. *J. Traffic Transp. Eng. Engl. Ed.* 12, 926–964. doi:10.1016/j.jtte.2024.09.006

Si, W., Zhang, B., Zhang, X., Xia, W., Cheng, X., Luo, X., et al. (2024). Maximizing the circularity of asphalt pavements by improving the RAP content in recycled asphalt mixtures. *Constr. Build. Mater.* 438, 137316. doi:10.1016/j.conbuildmat.2024.137316

Sun, Y., Zhang, F., Wang, D., Chen, W., and Cannone Falchetto, A. (2026). Study on the multiple recycling limit of asphalt binders containing high RAP content based on chemical and rheological properties. *Fuel* 405, 136708. doi:10.1016/j.fuel.2025.136708

Wang, H. (2021). *Crumb rubber modified bitumen: experimental characterization and modelling*. Delft University of Technology. doi:10.4233/uuid:36295f09-923e-4c89-aecc-55994deb2e65

Wang, H., Liu, X., Apostolidis, P., Van De Ven, M., Erkens, S., and Skarpas, A. (2020a). Effect of laboratory aging on chemistry and rheology of crumb rubber modified bitumen. *Mater. Struct.* 53, 26. doi:10.1617/s11527-020-1451-9

Wang, H., Liu, X., Van De Ven, M., Lu, G., Erkens, S., and Skarpas, A. (2020b). Fatigue performance of long-term aged crumb rubber modified bitumen containing warm-mix additives. *Constr. Build. Mater.* 239, 117824. doi:10.1016/j.conbuildmat.2019.117824

Wang, X., Ma, B., Yu, M., Mao, W., and Si, W. (2025). Testing and modeling of incomplete phase change heat storage and release of epoxy resin/microcapsule composite phase change materials for asphalt pavement. *J. Energy Storage* 105, 114672. doi:10.1016/j.est.2024.114672

WBCSD (2010). *End-of-life tires: a framework for effective management systems*. Geneva: World Business Council for Sustainable Development.

Zhang, F., Cannone Falchetto, A., Wang, D., Li, Z., Sun, Y., and Lin, W. (2025a). Prediction of asphalt rheological properties for paving and maintenance assistance using explainable machine learning. *Fuel* 396, 135319. doi:10.1016/j.fuel.2025.135319

Zhang, F., Zhu, J., Sun, Y., Mariam Benny, C., Wang, D., and Cannone Falchetto, A. (2025b). Effect analysis of using tall oil pitch (TOP) to partially extend bitumen in asphalt pavements: comparison of different TOPs. *Road Mater. Pavement Des.* 26, 361–380. doi:10.1080/14680629.2025.2483478